

Investigation the Crystalline Size and Strain of Perovskite ($\text{YBa}_2\text{Cu}_3\text{O}_{6+\sigma}$) by variant method

Mustafa K. Kamil¹, Kareem A. Jasim²

^{1,2} University of Baghdad, College of Education, Ibn -Al-Haithem, Department of Physics, Iraq.
Corresponding author: Contact:Mustafa.khaled1104a@ihcoedu.uobaghdad.edu.iq

Article Info

Volume 83

Page Number: 8719 - 8723

Publication Issue:

May - June 2020

Article History

Article Received: 19 November 2019

Revised: 27 January 2020

Accepted: 24 February 2020

Publication: 18 May 2020

Abstract:

The Perovskite compound of $\text{YBa}_2\text{Cu}_3\text{O}_{6+\sigma}$, in this study was prepared by method of pulsed laser deposition (PLD) on substrate of quartz. The diffraction of X-RAY was studied on the nature of crystalline of the compound $\text{YBa}_2\text{Cu}_3\text{O}_{6+\sigma}$, the results showed Crystal system tetragonal structures. The Full width at half maximum (FWHM) was calculated by the Orange Pro program by using X-RAY data. The crystalline size and stress were calculated by Scherrer, Willeamson-Heall, size-strain-plot and Halder-Wgner methods, Where the average of crystalline size and stress (65.66 nm , 5.827×10^{-3}), respectively.

Keywords: $\text{YBa}_2\text{Cu}_3\text{O}_{6+\sigma}$, Scherrer, Halder-Wagner, Williamson-Hall, size-strain plot.

Introduction:

$\text{YBa}_2\text{Cu}_3\text{O}_7$ is a compound of Perovskite, which are considered a ceramic material, they are characterized by abundance. Depending on the atoms / molecules used in the structure [1]. Perovskite can have an impressive array of interesting properties, including superconductivity, giant magneto resistance, spin-dependent transport (spintronics) and catalytic properties. Perovskite are an exciting stadium for physicists, chemists, and material scientists [2]. Its applications extend to energy production, environmental containment and waste contained in radioactive waste containers. Radioactive waste encapsulation, communications resonant insulating materials [3]. Perovskite and its molecular formula SrTiO_3 . Perovskite was first discovered in 1839 in the Ural Mountains in Russia and named this name after the Russian metallurgist Lev Percevsy. It is a substance that has a special crystal structure. The Perovskite composition possesses a general quantitative chemical formula (ABX_3), where (A) and (B) are positive ions (Cations) and the negative ion (Anion). Positive ions (A) and (B) may be It possesses a variety of charges, and the original mineral Perovskite composition is (CaTiO_3) and it

has a positive ion (A) represented by calcium (Ca) and has two valence while the positive ion (B) represented by titanium (Ti) has a trivalent valence. The traditional Perovskite network view includes the small positive ion (B) within the octahedral reticular structure of oxygen, while the large positive ion (A) is surrounded by symmetry number (12) oxygen atoms [4, 5].

2.Experimental technique:

The synthesis of $\text{YBa}_2\text{Cu}_3\text{O}_7$ compounds have been prepared by Thin film method .We have used appropriate weights of pure powders materials 99% of Y_2O_3 , BaO and CuO as starting materials. As the mixing and grinding operations took place in two stages:

The first stage: was carried out using a manual mortar, where the process of grinding and mixing took place for a period of an hour.

The second stage: It was by a whirlpool electric mixer, using that steel balls for a period of (2 hr),the aim of this mechanism was to obtain accurate powders as well as to obtain the best uniformity.

The mixture was dried in an oven at 150°C . In the second step the mixture was pressed into disc shaped pellets (15 mm) in diameter and (3-4 mm)

thick, using hydraulic press under pressure of (7.5 ton/cm²). The disk was then used to preparation the sample by pulsed laser deposition (PLD) on a quartz substrate, at a pressure of 10⁻⁴ torr and at a rate of 400 beats per minute for three minutes. Then it is put in farness for calcinations at 800°C during 24hr. With a heating rate of (10 C / min) and under normal atmospheric pressure, in order to obtain coherent samples in order to ensure an optimal spread process between the atoms, then the samples were cooled to room temperature and at a cooling rate (10 C / min). The structure of the prepared sample was obtained by using x-ray diffract meter (XRD). By using the Shimadzu X-ray Inspector with specifications (CuK α , Voltage: 40Kv, Current: 30mA, Wave Length: 1.5406Å) and within the range (10°-80°) with a step size of 0.02° and at room temperature. Then the results of X-RAY for the sample are compared by using the match program to ensure that the required compound has been obtained.

3. Discussion of the results

The diffraction of X-RAY for compound YBa₂Cu₃O_{6+ σ} , in the range of 10° < 2 θ < 80° shows peaks at (22.83°, 24.78°, 27.57°, 30.57°, 32.70°, 33.83°, 36.37°, 38.26°, 40.29°, 46.88°, 50.98° and 68.17°). Corresponding to the planes (100), (101), (012), (004), (103), (111), (112), (014), (113), (200), (213), and (206), respectively. Figure 1 drawing by using the Match! Program, showing two phases:

The first phase (YBa₂Cu_{2.91}O_{5.8}) source COD (Crystallography Open Database) Link to orig. entry 1535083. Where the proportion of congruence with this phase was equal to (50.3 %) and Crystal system tetragonal [6].

The second phase (YBa₂Cu₃O₆) source COD (Crystallography Open Database) Link to orig. entry 1540272. Where the proportion of congruence with this phase was equal to (49.7 %) and Crystal system tetragonal [7].

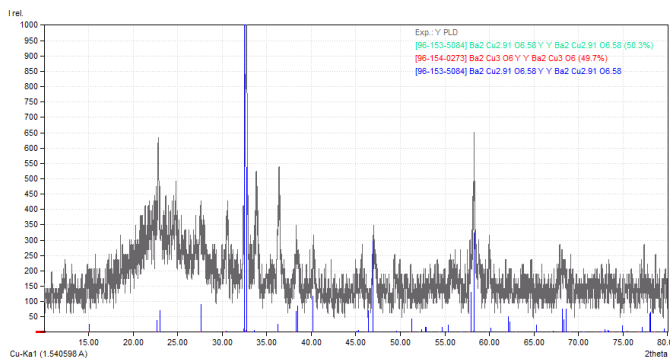


Fig. 1. XRD pattern of the compound

YBa₂Cu₃O_{6+ σ} drawing by using the Match! Program, with reference source COD (Crystallography Open Database) Link to orig. entry 1535083 and 1540272

3.1 Method of Scheirrir

Due to the crystalline size effect and intrinsic strain effect, the diffraction of X-RAD peak is larger in the crystals so this peak broadening usually consists of two sections of instrumental broadening and physical broadening. In order for the Scherrer method to be applied in a healthy way, it is very important to calculate the exact value of β_{hkl} accurately [8]. This instrumental broadening can be corrected using the following relation,

$$\beta_{hkl} = [(\beta_{hkl}^2)_m - (\beta_{hkl}^2)_i]^{1/2} \quad (1)$$

Where β_{hkl} is the corrected broadening, $(\beta_{hkl})_m$ is the measured broadening and $(\beta_{hkl})_i$ is the instrumental broadening. Calculation of the mean crystalline size using the Scherer equation [9,10]:

$$D = \frac{k\lambda}{\beta_{hkl} \cos \theta} \quad (2)$$

Where, D is a crystal size, k is a coefficient = 0.9; λ , X-ray wavelength = 1.540598 Å; θ is the Bragg angle. The equation (2) can be rewritten,

$$\cos \theta = \frac{k\lambda}{D} \cdot \frac{1}{\beta_{hkl}} \quad (3)$$

Now, plotting a graph of $1/\beta_{hkl}$ vs $\cos \theta$ for compound YBa₂Cu₃O_{6+ σ} , as shown in Fig.2, Where $1/\beta_{hkl}$ Represents the X axis and $\cos \theta$ Represents the Y axis, Through Figure 1, the crystalline size, which equals the slope, where it is found as 63.02 nm.

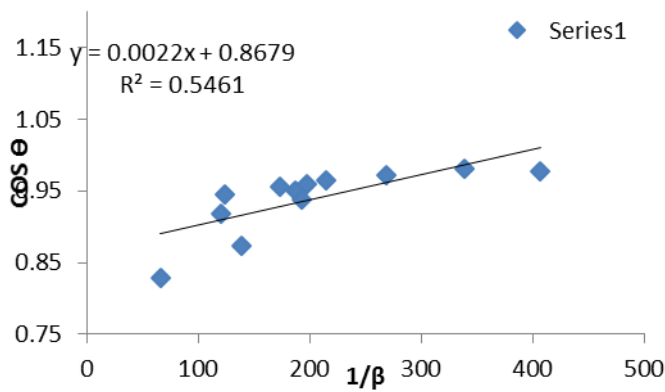


Fig. 2. Scherrer plot for compound $\text{YBa}_2\text{Cu}_3\text{O}_{6+\sigma}$.

0.0055. The average crystalline size of the compound $\text{YBa}_2\text{Cu}_3\text{O}_{6+\sigma}$ given by y-intercept, which is found as 64.49 nm.

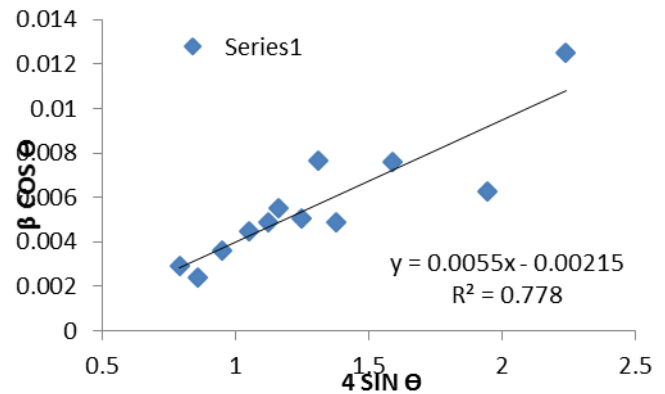


Fig. 3. Williamson-Hall (W-H) plot for compound $\text{YBa}_2\text{Cu}_3\text{O}_{6+\sigma}$.

3. 2 method of Willeamson-Heall

(W-H) method to find crystalline size and strain. Physical line broadening of the peak X-ray diffraction occurs due to the size and exact tension of the crystals. Thus, the total broadening due to strain and size in a particular peak having the hkl value, can be expressed as [10,11],

$$\beta_{hkl} = (\beta_{hkl})_{\text{size}} + (\beta_{hkl})_{\text{strain}} \quad (4)$$

The peak extending caused by strain can be represented by,

$$(\beta_{hkl})_{\text{strain}} = 4\epsilon \tan \theta \quad (5)$$

The β_{hkl} is the (FWHM) for diffraction planes different and the ϵ represents the strain [12].

$$\beta_{hkl} = \frac{k\lambda}{D \cos \theta} + 4\epsilon \tan \theta \quad (6)$$

When rearranging equation (6) we get,

$$\beta_{hkl} \cos \theta = \frac{k\lambda}{D} + 4\epsilon \sin \theta \quad (7)$$

The equation above is a straight line equation, now, plotting a graph of $4 \sin \theta$ vs $\beta_{hkl} \cos \theta$ for compound $\text{YBa}_2\text{Cu}_3\text{O}_{6+\sigma}$, as shown in Fig.3, where $4 \sin \theta$ Represents the X axis and $\beta_{hkl} \cos \theta$ Represents the Y axis. Slope of the equation of a straight line in Figure (3) gives the value of the intrinsic strain, which is found as

3. 3 Method of Size-strain plot (SSP)

The SSP method also gives a better isotropic broadening performance, as it puts greater focus on reflections at low angle, where precision are greater than in high angles. That is by reason of X-RAY data is of lower quality at low angles and peaks are typically heavily overlapped at low diffracting angles. Therefore, the SSP measurement is carried out will use the formula [13].As following

$$\frac{k\lambda}{D} \cdot [d_{hkl}^2 \cdot \beta_{hkl} \cdot \cos \theta] + \frac{\epsilon^2}{4} = [d_{hkl} \cdot \beta_{hkl} \cdot \cos \theta]^2 \quad (8)$$

Plotting a graph of $[d_{hkl}^2 \cdot \beta_{hkl} \cdot \cos \theta]$ vs $[d_{hkl} \cdot \beta_{hkl} \cdot \cos \theta]^2$ from the above equation is a straight line equation, as shown in Fig.4, where $[d_{hkl}^2 \cdot \beta_{hkl} \cdot \cos \theta]$ represents the X axis and $[d_{hkl} \cdot \beta_{hkl} \cdot \cos \theta]^2$ represents the Y axis.

The slope for an equation of the straight line provides the value of average crystalline size [10,14], which is found as 69.32 nm, while the intrinsic strain of the compound $\text{YBa}_2\text{Cu}_3\text{O}_{6+\sigma}$ given by y-intercept, which is found as 0.006325.

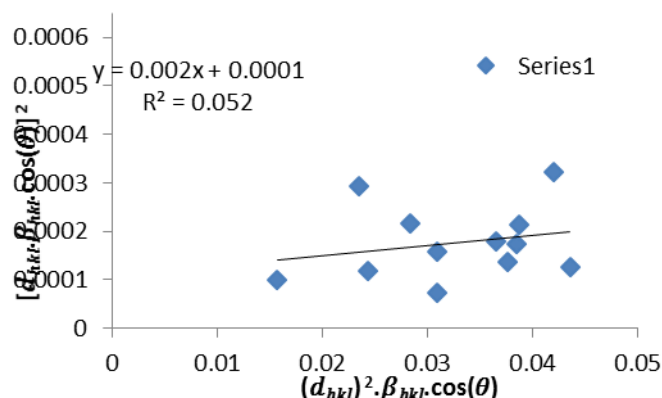


Fig. 4. Size-strain plot (SSP) plot for compound $\text{YBa}_2\text{Cu}_3\text{O}_{6+\sigma}$.

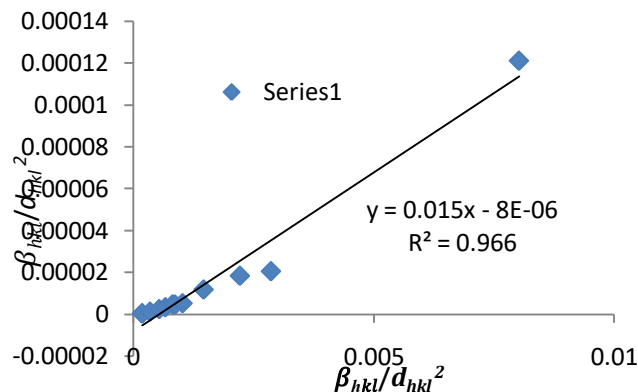


Fig. 5. Halder-Wagner plot for compound $\text{YBa}_2\text{Cu}_3\text{O}_{6+\sigma}$.

3.4 Method of Halder-Wagner

This method has the advantage that the peaks in low and medium angle ranges are given more weight, where the overlap of the diffracting peaks is much less. Now, according to the Halder-Wagner process, the Relationship between crystalline size and lattice strain is given by [15,16],

$$\left(\frac{\beta_{hkl}}{d_{hkl}}\right)^2 = \frac{1}{D} \left(\frac{\beta_{hkl}}{d_{hkl}}\right) + \left(\frac{\varepsilon}{2}\right)^2 \quad (9)$$

The equation above is a straight line equation, now, plotting a graph of $\left(\frac{\beta_{hkl}}{d_{hkl}}\right)^2$ vs $\left(\frac{\beta_{hkl}}{d_{hkl}}\right)$, as shown in Fig.5, where $\left(\frac{\beta_{hkl}}{d_{hkl}}\right)$ represents the X axis and $\left(\frac{\beta_{hkl}}{d_{hkl}}\right)^2$ represents the Y axis [17]. The slope of this straight line gives the value of average crystalline size, which is found as 65.78 nm.

The intrinsic strain of the compound $\text{YBa}_2\text{Cu}_3\text{O}_{6+\sigma}$ given by y-intercept, which is found as 0.005657.

The table (1) appears. That almost all of the calculation results are the same except for the SSP method, Since the XRD peak profile size expansion was considered as a Lorentzian function, there is very little difference, although Strain expansion is the Gaussian function. In fact, however, the XRD peak is neither the Lorentzian function nor the Gaussian function, since the XRD peak region suits the Gaussian function well, while its tail falls very quickly without matching, At the other hand, in the Lorentz function, the profile tail is well suited, but this does not correspond to the XRD peak area [18].

Table (1) geometrical parameters of compound $\text{YBa}_2\text{Cu}_3\text{O}_{6+\sigma}$ using different Models.

Scherrer	Williamson-Heall	Size-Strain Plot	Halder-Wagner
D (nm)	D (nm) ε	D (nm) ε	D (nm) ε
63.02	64.49 0.0055	69.32 0.006325	65.78 0.005657

CONCLUSION

We have successfully prepared the compound of Perovskite $\text{LaBa}_2\text{Cu}_3\text{O}_{6+\sigma}$ was prepared by the pulsed laser deposition method (PLD) on the quartz substrate. Scherrer's method recognizes only the influence of crystalline size for XRD peak

broadening, but says nothing about the microstructures of the lattice (W-H) system simply assuming peak broadening like a function of diffraction angle (2θ), which is expected to have been a combination for size induced broadening with strain induced broadening. While (SSP) method, which deals with the peak profiles analysis. The (H-W) method is built on assuming peak broadening is a symmetrical Voigt function [19].

REFERENCES

1. Szuromi, Phillip; Grocholski, "Natural and engineered perovskites". (2017).
2. Wenk, Hans-Rudolf; Bulakh, Andrei. "Minerals Their Constitution and Origin". Cambridge University Press. (2004).
3. Inoue, Naoki and Zou, Yanhui, "Physical properties of perovskite type lithium ionic conductor", (2006).
4. H.Eschrig "Theory of Superconductivity" (2008).
5. M.A. Omar, "Elementary solid state physics", 5th ed., Addison – Wesley, (1993).
6. Sorokina N.I., Molchanov V.N., Tamazyán R.A., Makarova N.G., Shcherbakova L.G., Nikolaevskii A.N., Pigal'skii K.S., Sirota M.I., Simonov V.I., "Specific features of HTSC YBa₂Cu₃O_{6.58} single crystals", *Kristallografiya* 38, 61-67 (1993).
7. Klamut J., Janczak J., Henkie Z., Glovyak T., Zygmunt A., Horyn R., Kubiak R., Bukowski Z., Wojakowski A., Lukaszewicz K., Stepen'-Damm Yu., "Thermal vibrations in Y Ba₂ Cu₃ O_{6+x} and Pr Ba₂ Cu₃ O_{6+x}", *Acta Physica Polonica*, A 73, 759-765 (1988).
8. R. Yogamalara, R. Srinivasan, A. Vinu, K. Ariga, A.C. Bose, X-ray peak broadening analysis in ZnO nanoparticles, *Solid State Commun*, (2009).
9. Paul A .Tipler and Ralph A . Liewellyn , "Modern physics " fourth Edition , freeman New York , pp 487 - 495 , (2002).
10. Nath, Debojyoti, Fouran Singh, and Ratan Das. "X-ray diffraction analysis by Williamson-Hall, Halder-Wagner and size-strain plot methods of CdSe nanoparticles-a comparative study." *Materials Chemistry and Physics* 239 (2020): 122021.
11. Barsoum M. W, "Fundamentals of Ceramics", university of Oxford UK Iop publishing Ltd, pp 304 - 306, (2003).
12. Vijaya Kumar K and Sreekanth T "Solid State Physics" Chand &company Ltd, New Delhi, (2005).
13. V.D. Mote, Y. Purushotham, B.N. Dole, Williamson-Hall analysis in estimation of lattice strain in nanometer-sized ZnO particles, *J. Theor. Appl. Phys.* (2012).
14. Ali M .Omer, "Elementary Solid State physics" fifth Impression, Dorling Kindersley Ltd, pp 372 - 380, (2009).
15. Bolton W, "Engineering Materials Technology", 3rd ed, Butterworth-Heine-mann , Oxford , p 293 , (1998).
16. Brian S. Mitchell "An Introduction To Materials Engineering and Science" John Wiley & sons, (2004).
17. W.B. Michel, "Fundamentals of ceramics", 1st edition, Mc. Grow-Hill Book, Inc. New York. (1997).
18. D. Balzar, H. Ledbetter, Voigt-function modeling in fourier analysis of size- and strain-broadened X-ray diffraction peaks, *J. Appl. Crystallogr.* 26 (1) (1993).
19. W.H. Hall, X-ray line broadening in metals, *Proc. Phys. Soc. Sect. A* 62 (11) (1949).